A&A 505, 601–604 (2009)
DOI: 10.1051/0004-6361/200912820

Astronomy & Astrophysics

The host galaxy of 3C 279
(Research Note)

K. Nilsson[1], T. Pursimo[2], C. Villforth[1,2], E. Lindfors[1], and L. O. Takalo[1]

[1] Tuorla Observatory, Department of Physics and Astronomy, University of Turku, Väisäläntie 20, 21500 Piikkiö, Finland
e-mail: kani@utu.fi
[2] Nordic Optical Telescope, Apartado 474, 38700 Santa Cruz de La Palma, Spain

Received 3 July 2009 / Accepted 9 August 2009

ABSTRACT

We have obtained a deep *i*-band image of the blazar 3C 279 while the target was in a low optical state. Due to the faintness of the optical nucleus we have made the first detection of the host galaxy. The host galaxy has an apparent *I*-band magnitude of 18.4 ± 0.3 and an effective radius of (2.7 ± 1.1) arcsec. The luminosity of the host galaxy $M_R = -23.8$ is consistent with the luminosities of other radio-loud quasar host galaxies. Using the empirical correlation between bulge luminosity and central black hole mass $M_{\rm bh}$ we estimate $\log(M_{\rm bh}/M_\odot) = 8.9 \pm 0.5$, broadly consistent with values obtained by photoionization methods.

Key words. galaxies: active – quasars: individual: 3C 279 – galaxies: nuclei

1. Introduction

The host galaxies of active galactic nuclei (AGN) provide important information of the environment and evolution of their central black holes. The close connection between the central black holes and their host galaxies is clearly manifested by the correlations between the central black hole mass $M_{\rm bh}$ and the host galaxy parameters, such as the central velocity dispersion σ (Ferrarese & Merritt 2000; Gebhardt et al. 2000; Merritt & Ferrarese 2001), bulge mass $M_{\rm bulge}$ (Magorrian et al. 1998) and galaxy light concentration $C_{\rm re}(1/3)$ (Graham et al. 2001). It is usually much easier to determine the host galaxy parameters than to apply kinematic methods or reverberation mapping (e.g. Kaspi et al. 2000) making the host galaxy method an appealing alternative to estimate black hole masses in galaxies. Host galaxies can also be used to study the unified schemes of AGN since their properties do not depend on viewing angle (Urry & Padovani 1995).

3C 279 ($z = 0.538$) is an AGN which belongs to the class of blazars, whose most notable features are strong continuum radiation and high variability over the whole electromagnetic spectrum and high optical and radio polarization. The blazar class comprises of flat spectrum radio quasars (FSRQs) and BL Lacertae objects (BL Lacs) whose main difference in the optical lies in the strength of their broad emission lines: the latter group has very weak or nonexistent emission lines whereas in the former they are more pronounced. 3C 279 is classified as a FSRQ, although both the emission line strengths and γ-ray properties place it close to the FSRQ-BL Lac border (Koratkar et al. 1998; Ghisellini et al. 2009).

Despite of 3C 279 being subject to intensive study over the last three decades, determining its host galaxy parameters has received little attention. The only published host galaxy study was made by Kotilainen et al. (1998) who observed 3C 279 in the *H*-band, but could only derive an upper limit of $H > 13.7$ for the host galaxy. One of the main factors affecting the host galaxy detection efficiency is the nucleus to host ratio: when the nucleus is very bright compared to the host galaxy its is difficult to detect the host galaxy, let alone reliably determine its main parameters (magnitude and effective radius). 3C 279 is known to be highly variable in the optical bands with historical variations over 6 mag in the *B*-band (Webb et al. 1990). The rapid variability of 3C 279 makes the host galaxy detection even more challenging as is it difficult to observe the target in a low state.

We are currently monitoring over 40 blazars in the *R*-band in the Tuorla Observatory blazar monitoring program[1]. In the end of June 2008 we observed 3C 279 to go into a fairly deep optical minimum ($R \sim 16.8$) and initiated prompt *i*-band imaging at the Nordic Optical Telescope (NOT) to detect its host galaxy. The results of this imaging are presented in this research note.

Throughout this paper we use the cosmology $H_0 = 70\ \mathrm{km\,s^{-1}\,Mpc^{-1}}$, $\Omega_M = 0.3$ and $\Omega_\Lambda = 0.7$.

2. Observations and data reduction

The observations were made in June 23, 24, 2008 with the Nordic Optical Telescope (NOT) using the ALFOSC instrument. This instrument has a pixel scale of 0.″189/pixel and a gain of 0.726 e^-/ADU and a readout noise of 3.2 electrons. The field of view of the instrument is $6.5' \times 6.5'$. Altogether 24 images of the 3C 279 field were obtained through an *i*-band filter with almost an uniform transmission between 725 and 875 nm. Individual exposure times were kept low enough (100–200 s) to leave 3C 279 and a nearby star (star 1 in Fig. 1) unsaturated. The position of 3C 279 on the CCD was changed between exposures to be able to make a fringe correction image.

[1] http://users.utu.fi/~kani/1m/index.html

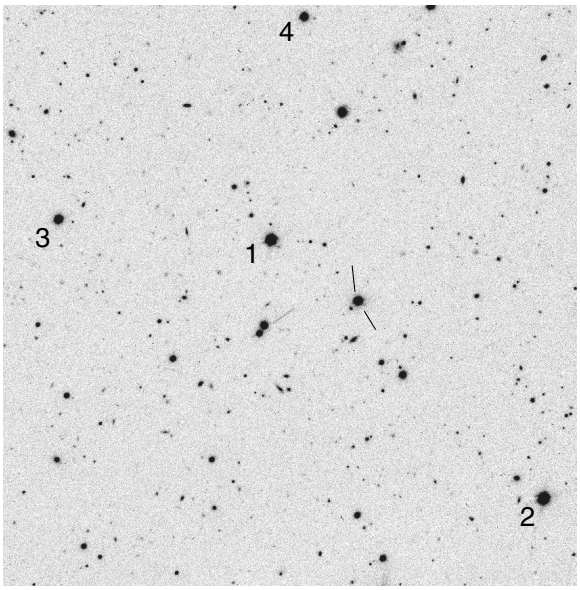

Fig. 1. The summed *i*-band image of the field around 3C 279. The field size is 5.3′ × 5.4′, *North is up and East is to the left*. Stars 1−4 are discussed in the text.

The individual images were first bias-subtracted and then flat-fielded with twilight flats in the usual way using IRAF[2]. The fringe pattern visible in the images was corrected by subtracting a fringe correction image produced by median combining all 24 images and applying simultaneously a sigma clipping cut to the pixel intensity values. After correction for the fringe pattern, the individual frames were registered and summed. The summed image shown in Fig. 1 has a *FWHM* of 0.79 arcsec and a total exposure time of 3300 s.

Calibration of the field was obtained via star 1 in Fig. 1, for which Smith & Balonek (1998) give $I = 15.00 \pm 0.04$. Since the *i*-band filter used in our observations closely matches the Cousins *I*-band filter, we expect only small color effects between our *i*-band magnitudes and standard *I*-band magnitudes. We conservatively estimate the error of calibration to be 0.1 mag.

3. Analysis and results

We looked for the host galaxy of 3C 279 by fitting two-dimensional surface brightness models to the observed *i*-band image. We used three different models: an unresolved nucleus only, nucleus + a de Vaucouleurs profile host galaxy (Sérsic $\beta = 0.25$) and nucleus + a disk host galaxy ($\beta = 1.0$). Details of this fitting process can be found in Nilsson et al. (1999). In short, the model has three adjustable parameters, the magnitude of the nucleus $I_{\rm core}$, the magnitude of the host galaxy $I_{\rm host}$ and the effective radius of the host galaxy $r_{\rm eff}$. The unresolved nucleus is assumed to be centered on the host galaxy. The three parameters are adjusted via an iterative Levenberg-Marquardt loop until the minimum chi squared between the model and the observed surface brightness distribution is found. The fit was extended to an outer radius of 9.″5, except that the pixels affected by a galaxy 5.″9 SE of 3C 279 were masked out from the fit.

[2] IRAF is distributed by the National Optical Astronomy Observatories, which are operated by the Association of Universities for Research in Astronomy, Inc., under cooperative agreement with the National Science Foundation.

Table 1. The results of the model fitting.

Model	$I_{\rm core}$	$I_{\rm host}$	$r_{\rm eff}$	χ^2/d.o.f.
Nucleus	15.99			1.38
Nucleus + De V.	16.13	18.43	2.″7	1.03
Nucleus + disk	16.08	19.04	2.″8	1.05

Prior to computing the chi squared the model was convolved with the PSF. We used star 1 in Fig. 1 for the PSF due to its high signal to noise and proximity to 3C 279. As in Nilsson et al. (2008), we studied the variability of the PSF across the FOV by extracting the surface brightness profiles of stars 1−4 in Fig. 1 and deriving the rms scatter between the profiles. The PSF variability was then parameterized by a parabolic expression

$$\sigma_{\rm PSF}(r) = 0.035 + 2 \times 10^{-5} \cdot r^2, \quad (1)$$

where $\sigma_{\rm PSF}(r)$ is the uncertainty in the PSF relative to the intensity at radius r (pixels) from the PSF center. We then computed the expected variance σ^2 in a pixel with intensity I (ADU) and distance r from the center of 3C 279 from the expression

$$\sigma^2 = \frac{G * I + R^2}{G^2} + [\sigma_{\rm PSF}(r) * I]^2, \quad (2)$$

where G is the effective gain and R is the effective readout noise, and compute the χ^2 from

$$\chi^2 = \sum_i \frac{(I_i - M_i)^2}{\sigma_i^2}, \quad (3)$$

where M is the model intensity and the summation is over all unmasked pixels within the fitting radius. By including the PSF variability into the computation of χ^2 we can ensure that the results are not dominated by PSF errors, which are most pronounced close to the center of the object.

The results of this model fitting are summarized in Table 1 and Fig. 2. We see a clear excess in 3C 279 over the PSF and this excess is clearly above any PSF variability across the FOV (see the lower panel of Fig. 2). The models with a host galaxy give a much better fit than a model with pure nucleus with χ^2 indicating a near-perfect fit. The model with a de Vaucouleurs host galaxy gives a slightly better fit that the model with a disk galaxy but the difference is not significant according to our error simulations (see below). However, since the de Vaucouleurs profile gave formally a better fit and no blazar host galaxy has ever been associated with a disk galaxy, we concentrate in the following to the results with the de Vaucouleurs profile.

We have studied the sensitivity of the results to random noise, PSF variability and errors in the assumed profile of the host galaxy by performing 50 model fits to simulated images of 3C 279. In these simulations $I_{\rm core}$, $I_{\rm host}$ and $r_{\rm eff}$ were held constant at the values shown in Table 1, but the contribution from the different noise sources changed from one simulation to another.

The random noise in these simulations is assumed to raise from readout and photon noise according to the first term on the right hand side of Eq. (2). To model the PSF variability we created two PSF models in each simulation, slightly differing from each other. The simulated model was convolved with the first PSF and the model fits were made with the second PSF. Both PSFs consisted of an elliptical Moffat profile with $\beta = 2.5$. The ellipticity of the first PSF was randomly drawn from an uniform distribution with a minimum of 0.0 and a maximum of 0.12 and

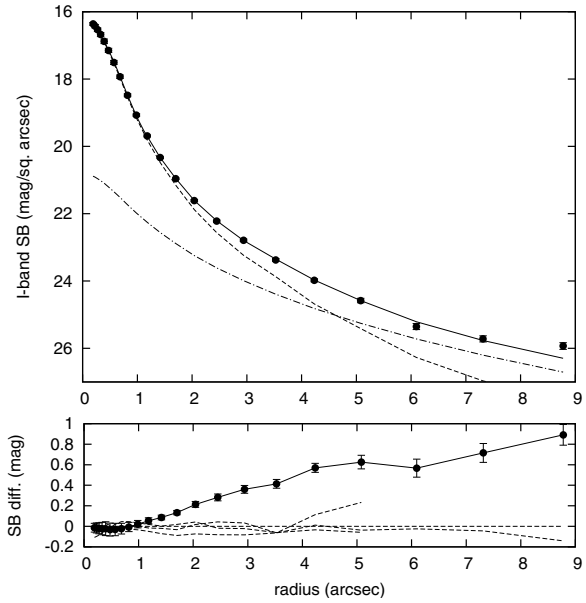

Fig. 2. *Upper panel*: the surface brightness profile of 3C 279 (filled symbols) together with the model (solid line), the nucleus (dashed line) and the host galaxy (dot-dashed line). *Lower panel*: the surface brightness profiles of 3C 279 (solid line and filled symbols) and stars 1−4 in Fig. 1 relative to star 1. Each profile is traced out to a radius where the surface brightness can be determined to better that 10% accuracy. Note that star 1 is represented by a horizontal line at SB = 0.0 in the *lower panel*.

the position angle from an uniform distribution between 0 and 180 degrees. For the second PSF the ellipticity was drawn from a Gaussian distribution with a mean equal to the ellipticity of the first PSF and $\sigma = 0.05$. The position angle of the second PSF was similarly drawn from a Gaussian distribution with a mean equal to the first PSF and $\sigma = 12.5$ degrees. The limits and standard deviations above were chosen to mimic the range of PSF shapes seen in our *i*-band images and to roughly reproduce the residuals seen in the model subtracted image of 3C 279.

We also included in the simulations the possibility that the host galaxy does not exactly follow the de Vaucouleurs profile with the slope of the surface brightness profile β equal to 0.25, as often is observed (e.g. Nilsson et al. 1999). Therefore, when creating the host galaxy model the profile slope β of the host galaxy was drawn from a Gaussian distribution with mean = 0.25 and $\sigma = 0.06$. When performing the fits to the simulated images the β parameter was held constant at 0.25, however.

After completing the simulations we computed the standard deviations of $I_{\rm core}$, $I_{\rm host}$ and $r_{\rm eff}$ to be 0.02 mag, 0.18 mag and 1.1 arcsec, respectively. Taking into account the error in the calibration we end up with $I_{\rm host} = 18.4 \pm 0.3$ and $r_{\rm eff} = 2.7 \pm 1.1$ arcsec for the host galaxy. The χ^2 in the simulated fits had an average of 1.11 and standard deviation $\sigma = 0.08$. Given that the scatter in χ^2 in the simulations is significantly larger than the difference in χ^2 between the de Vaucouleurs and disk models, we conclude that we cannot claim either of the two models to be significantly better.

4. Discussion

Since most host galaxy parameters and correlations have been discussed in the *R*-band we first convert the host galaxy magnitude from *I*-band to *R*-band. For the conversion we used

Table 2. Previous black hole mass determinations for 3C 279.

$\log(M_{\rm bh}/M_\odot)$	Method	Ref.
8.912	*FWHM* (H_β) − $L_{\rm opt}$	1
9.099	*FWHM* (H_β) − $L_{\rm opt}$	2
8.43	*FWHM* (H_β) − $L_{\rm opt}$	3
8.6	γ-ray luminosity	4
8.48	*FWHM* (H_β) − $L_{\rm opt}$	5
9.79	*FWHM* (H_β) − $L_{\rm opt}$	6
8.28	*FWHM* (H_β) − $L_{\rm opt}$	7

References: (1) Gu et al. (2001); (2) Cao & Jiang (2002); (3) Woo & Urry (2002); (4) Liang & Liu (2003); (5) Wang et al. (2004); (6) Bian & Zhao (2004); (7) Liu et al. (2006).

$A_I = 0.06$ for the galactic extinction (Schlegel et al. 1998), $K_I + e(I) = 0.4$ for the *K*-correction and evolutionary correction, based on Maraston (1998) and Maraston & Thomas (2000) and assuming galaxy formation at $z = 2$ and finally $R - I = 0.7$ for an elliptical galaxy (Fukugita et al. 1995). Using these values we derive $R = 18.7$ for the host galaxy of 3C 279, which translates into $M_R = -23.8$ in the adopted cosmology. This value is in the bright end of the values found for the host galaxies of radio-loud quasars (-23.2 ± 0.3, Dunlop et al. 2003, transferred to the cosmology used here) and BL Lacertae objects (-22.9 ± 0.5, Sbarufatti et al. 2005). The effective radius is (17 ± 7) kpc, which is fairly large compared to typical effective radii (∼10 kpc) found for radio-loud quasars and BL Lacs, although the margin of error is also large. Next we estimate the central black hole mass of 3C 279 using the relationship between bulge luminosity and central black hole mass derived in Bentz et al. (2009) using the same cosmology as here: $\log(M_{\rm bh}/10^8\ M_\odot) = -0.02 + 0.8\log(L_{\rm bulge}/10^{10}\ L_\odot)$, where $L_{\rm bulge}$ is measured in the V-band This relationship was derived using 26 Seyfert 1 galaxies and quasars at $z < 0.3$. Although the redshift of 3C 279 is outside this range, the host galaxy luminosity of 3C 279 is within the range of *V*-band bulge luminosities probed by this study $9 < \log(L_{\rm bulge}/L_\odot) < 11.5$.

As blazar host galaxies are expected to be bulge-dominated systems we use the derived *R*-band magnitude directly for computing the bulge luminosity. We first transferred the *R*-band luminosity of the host galaxy to the *V*-band using $V - R = 0.6$ (Fukugita et al. 1995) and used the above relation to derive $\log(M_{\rm bh}/M_\odot) = 8.9$ for 3C 279. The scatter in the $L_{\rm bulge} - M_{\rm bh}$ relation is ∼0.4 dex. The uncertainty arising from the host galaxy magnitude error is smaller (<0.2 dex), so our estimate of the black hole mass has a total error of ∼0.5 dex. Like the host galaxy luminosity, the derived black hole mass is in the upper end of the black hole mass distribution of FSRQs, but still consistent with the total observed range (see e.g. Ghisellini & Tavecchio 2008).

We have looked in the literature for other black hole mass determinations for 3C 279. The results of this search are summarized in Table 2. It is beyond the scope of this paper to discuss in detail the various methods used to derive the values in Table 2 and their relative merits. Most of them have been determined with the empirical *FWHM* (H_β) − $L_{\rm opt}$ correlation (e.g. Wandel et al. 1999) with different assumptions of BLR geometry. There is a broad range of values found by different authors, but most of them are in the range $8.5 < \log(M_{\rm bh}/M_\odot) < 9.0$, broadly consistent with the value found here. The two last values in Table 2 deviate most from the general consensus and at least in Bian & Zhao (2004) (ref. 6 in Table 2) the high $M_{\rm bh}$ estimate can be

traced to a much broader reported H_β line width than the other authors.

5. Summary

The results of this paper can summarized as follows:

1. We have obtained a deep *i*-band image of 3C 279 which has enabled us to reveal the host galaxy for the first time.
2. The luminosity of the host galaxy ($M_R = -23.8$) is in the bright end of luminosities of other radio-loud quasar host galaxies. The derived effective radius (17 ± 7 kpc) is quite large compared to other radio-loud quasars, but the effective radius is not very well constrained.
3. Using the empirical correlation between bulge luminosity and central black hole mass $M_{\rm bh}$ we estimate $\log(M_{\rm bh}/M_\odot) = 8.9 \pm 0.5$, broadly consistent with values obtained by photoionization methods.

Acknowledgements. The authors thank Talvikki Hovatta for useful discussions during the preparation of this paper. These data are based on observations made with the Nordic Optical Telescope, operated on the island of La Palma jointly by Denmark, Finland, Iceland, Norway, and Sweden, in the Spanish Observatorio del Roque de los Muchachos of the Instituto de Astrofisica de Canarias. The data presented here have been taken using ALFOSC, which is owned by the Instituto de Astrofisica de Andalucia (IAA) and operated at the Nordic Optical Telescope under agreement between IAA and the NBIfAFG of the Astronomical Observatory of Copenhagen.This research has made use of the NASA/IPAC Extragalactic Database (NED) which is operated by the Jet Propulsion Laboratory, California Institute of Technology, under contract with the National Aeronautics and Space Administration.

References

Bentz, M. C., Peterson, B. M., Pogge, R. W., & Vestergaard, M. 2009, ApJ, 694, L166
Bian, W., & Zhao, Y. 2004, MNRAS, 347, 607
Cao, X., & Jiang, D. R. 2002, MNRAS, 331, 111
Dunlop, J. S., McLure, R. J., Kukula, M. J., et al. 2003, MNRAS, 340, 1095
Ferrarese, L., & Merritt, D. 2000, ApJ, 539, L9
Fukugita, M., Shimasaku, K., & Ichikawa, T. 1995, PASP, 107, 945
Gebhardt, K., Bender, R., Bower, G., et al. 2000, ApJ, 539, L13
Ghisellini, G., & Tavecchio, F. 2008, MNRAS, 387, 1669
Ghisellini, G., Maraschi, L., & Tavecchio, F. 2009, MNRAS, 396, L105
Graham, A. W., Erwin, P., Caon, N., & Trujillo, I. 2001, ApJ, 563, L11
Gu, M., Cao, X., & Jiang, D. R. 2001, MNRAS, 327, 1111
Kaspi, S., Smith, P. S., Netzer, H., et al. 2000, ApJ, 533, 631
Koratkar, A., Pian, E., Urry, C. M., & Pesce, J. E. 1998, ApJ, 492, 173
Kotilainen, J. K., Falomo, R., & Scarpa, R. 1998, A&A, 332, 503
Liang, E. W., & Liu, H. T. 2003, MNRAS, 340, 632
Liu, Y., Jiang, D. R., & Gu, M. F. 2006, ApJ, 637, 669
Magorrian, J., Tremaine, S., Richstone, D., et al. 1998, AJ, 115, 2285
Maraston, C. 1998, MNRAS, 300, 872
Maraston, C., & Thomas, D. 2000, ApJ, 541, 126
Merritt, D., & Ferrarese, L. 2001, ApJ, 547, 140
Nilsson, K., Pursimo, T., Takalo, L. O., et al. 1999, PASP, 111, 1223
Nilsson, K., Pursimo, T., Sillanpää, A., Takalo, L. O., & Lindfors, E. 2008, A&A, 487, L29
Sbarufatti, B., Treves, A., & Falomo, R. 2005, ApJ, 635, 173
Schlegel, D. J., Finkbeiner, D. P., & Davis, M. 1998, ApJ, 500, 525
Smith, P. S., & Balonek, T. J. 1998, PASP, 110, 1164
Urry, C. M., & Padovani, P. 1995, PASP, 107, 803
Wandel, A., Peterson, B. M., & Malkan, M. A. 1999, ApJ, 526, 579
Wang, J.-M., Luo, B., & Ho, L. C. 2004, ApJ, 615, L9
Webb, J. R., Carini, M. T., Clements, S., et al. 1990, AJ, 100, 1452
Woo, J.-H., & Urry, C. M. 2002, ApJ, 579, 530